Chemistry Research Journal, 2019, 4(1):85-100

Available online www.chemrj.org

Research Article

ISSN: 2455-8990
CODEN(USA): CRJHA5

A preliminary quantum chemical analysis of the relationships between electronic structure and 5-HT_{1A} and 5-HT_{2A} receptor affinity in a series of 8-acetyl-7-hydroxy-4-methylcoumarin derivatives

Juan S. Gómez-Jeria*, Nelson Gatica-Díaz

Quantum Pharmacology Unit, Department of Chemistry, Faculty of Sciences, University of Chile. Las Palmeras 3425, Santiago 7800003, Chile

Abstract We present the results of a quantum-chemical analysis of the relationships between electronic structure and 5-HT_{1A} and 5-HT_{2A} receptor binding affinity for a series of 8-acetyl-7-hydroxy-4-methylcoumarin derivatives. The KPG model coupled with DFT calculations at the 6-31G(d,p) level were employed. Two statistically significant results were obtained. The results are synthesized in the corresponding partial pharmacophores. The most important result suggests that an unsaturated ring is an almost sure target for the development of new compounds with affinity for both receptors.

Keywords 5-HT_{1A} receptor, 5-HT_{2A} receptor, QSAR, methylcoumarin, KPG method, Density Functional Theory, QSAR, DFT, serotonin

Introduction

Due to importance of the serotonergic group of receptors [1-4], our Unit has been searching for a longtime for relationships between the molecular structure and receptor affinity of several different molecules interacting with them [5-20]. These studies are the results of the fact that many serotonin receptor types and subtypes were discovered through time and that many molecules interact with one or more of them. Recently, we have focused our interest in the work of Ostrowska et al. who measured the 5-HT_{1A} and 5-HT_{2A} receptor affinities of a series of 8-acetyl-7-hydroxy-4-methylcoumarin derivatives [21]. The molecules studied showed a higher affinity for the 5-HT_{1A} receptor. They present an interesting feature that has never been analyzed in our Unit, which is the different length of the chain linking two groups of rings. This poses a serious problem to define a common structure for all them.
In this paper we present the results of a Density Functional Theory study of the relationships between the electronic structure of the abovementioned molecules and their 5-HT_{1A} and 5-HT_{2A} receptor affinities.

Methods, models and calculations

Selection of molecules and biological activities

The selected molecules are a group of 8-acetyl-7-hydroxy-4-methylcoumarin derivatives that were selected from the aforementioned study[21]. Their general formula and receptor affinity are displayed, respectively, in Fig. 1 and Table 2.

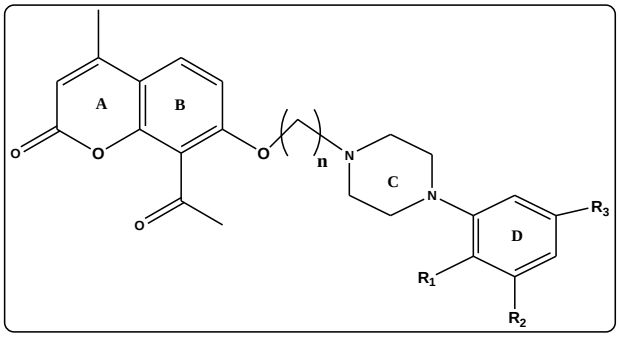

Figure 1: General formula of 8-acetyl-7-hydroxy-4-methylcoumarin derivatives

Table 1: 8-acetyl-7-hydroxy-4-methylcoumarin derivatives and biological activity

Mol.	n	R_1	R_2	R_3	$\log(K_i)$ 5-HT_{1A}	$\log(K_i)$ 5-HT_{2A}
1	3	Cl	H	H	0.30	1.34
2	3	H	CH_3	CH_3	-0.05	1.10
3	3	CH_3	H	CH_3	1.15	2.01
4	3	Br	H	H	-0.30	0.85
5	3	H	Br	H	0.54	0.78
6	3	H	F	H	3.13	2.61
7	3	CF_3	H	H	0.94	1.30
8	3	OCH_3	H	H	-0.22	0.90
9	4	Cl	H	H	-0.05	1.30
10	4	H	CH_3	CH_3	0.57	1.76
11	4	CH_3	H	CH_3	0.73	1.67
12	4	Br	H	H	0.18	1.00
13	4	H	Br	H	0.40	0.81
14	4	H	F	H	1.70	2.60
15	4	CF_3	H	H	1.04	1.69
16	4	OCH_3	H	H	0.00	1.75

Note that molecules 9-16 have a longer chain (n=4) linking rings B and C than molecules 1-8 (n=3).

Methods and Calculations

The method used to generate structure-affinity relationships is called the Klopman-Peradejordi-Gómez method (KPG). It was created by Peradejordi starting from the work of Klopman [22]. The model was expanded by Gómez-Jeria, who added about 14 local atomic reactivity indices derived from the Hartree-Fock scheme [23-26]. Initially, this method was employed only to analyze equilibrium (affinity) constants measured in different ways [5, 15, 17-19, 27-42]. A considerable progress was achieved when it was shown that the KPG method could be applied, with some strong restrictions, to any biological activity [40, 43-60].

The electronic structure of all molecules was calculated within the Density Functional Theory (DFT) at the B3LYP/6-31g(d,p) level after full geometry optimization [61] with the Gaussian suite of programs [62]. All the data used to calculate numerical values for the local atomic reactivity indices was obtained from the Gaussian results with the D-Cent-QSAR software [63]. All the electron populations smaller than or equal to 0.01 e were considered as zero. Negative electron populations coming from Mulliken Population Analysis were adjusted as habitual [64]. As the resolution of the system of linear equations is not possible because we have not sufficient molecules, we made use of Linear Multiple Regression Analysis (LMRA) techniques to find the most statistically significant solution. For each case, a matrix containing the dependent variable (the receptor affinity of each case) and the local atomic reactivity indices of all atoms of the common skeleton as independent variables was built. The Statistica software was used for LMRA [65].

We worked with the *common skeleton hypothesis* affirming that there is a certain collection of atoms, common to all molecules analyzed, that accounts for nearly all the biological activity [66]. The action of the substituents consists in modifying the electronic structure of the common skeleton (CS) and influencing the right alignment of the drug throughout the orientational parameters. It is hypothesized that different parts or this common skeleton accounts for almost all the interactions leading to the expression of a given biological activity. In Table 1 and Fig. 1 we can see that the chain linking rings B and C has two different lengths. We shall use the simplest hypothesis to build de common skeleton. Considering that the CS requires the same number of atoms, we employed as the 'common chain' the O-C-C fragment (attached to ring B, Fig. 1) and the carbon atom bonded to ring C. This approach is equivalent to state that if we overlap, for example, rings A-B of all molecules, then the chain linking rings C-D of molecules with n=4 in Table 1 must have a different conformation in such a way that rings C-D also coincide in all molecules. The resulting common skeleton for this case is shown in Fig. 2.

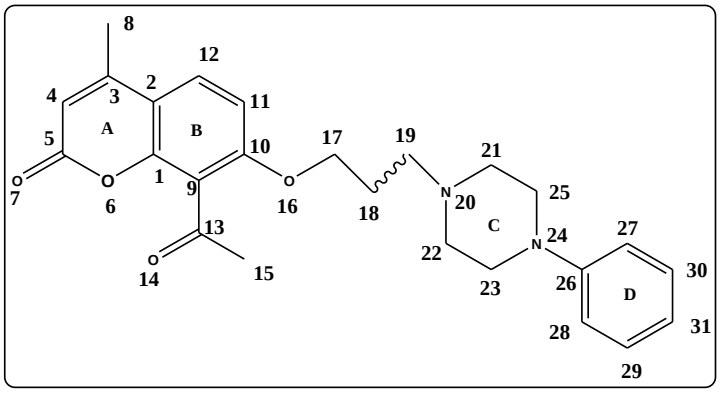

Figure 2: Common skeleton numbering

The molecular electrostatic potentials (MEP) were calculated with GaussView and Molekel [67, 68].

Results

Results for 5-HT$_{1A}$ receptor affinity

The best equation obtained was:

$$\log K_i = -9.07 + 55.98\mathrm{F}_{23}(\mathrm{LUMO}+1)^* + 1.80\eta_{23} - 2.37\mathrm{S}_{21}^{\mathrm{N}}(\mathrm{LUMO}+1)^* + \\ +0.66\mathrm{S}_{28}^{\mathrm{E}}(\mathrm{HOMO}-2)^* - 0.91\omega_{22} \quad (1)$$

with n=16, adj-R^2=0.96, F(5,10)=72.81 (p<0.000001) and SD=0.17. No outliers were detected and no residuals fall outside the ±2σ limits. Here,F_{23}(LUMO+1)* is the electron population of the second lowest empty MO localized on atom 23, η_{23} is the local atomic hardness of atom 23, S_{21}^{N}(LUMO+1)* is the nucleophilic superdelocalizability of the second lowest MO localized on atom 21, S_{28}^{E}(HOMO-2)* is the electrophilic superdelocalizability of the third highest occupied MO localized on atom 28 and ω_{22} is the local atomic electrophilicity of atom 22.Tables 2 and 3 show the beta coefficients, the results of the t-test for significance of coefficients and the matrix of squared correlation coefficients for the variables of Eq. 1. There are no significant internal correlations between independent variables (Table 3). Figure 3 displays the plot of observed *vs.* calculated log(K_i) values.

Table 2: Beta coefficients and t-test for significance of coefficients in Eq. 1

Variable	Beta	t(10)	p-level
F_{23}(LUMO+1)*	1.01	14.23	0.000000
η_{23}	0.31	3.82	0.003
S_{21}^{N}(LUMO+1)*	-0.55	-7.73	0.00002
S_{28}^{E}(HOMO-2)*	0.28	4.16	0.002
ω_{22}	-0.29	-3.61	0.005

Table 3: Matrix of squared correlation coefficients for the variables in Eq. 1

	F_{23}(LUMO+1)*	η_{23}	S_{21}^{N}(LUMO+1)*	S_{28}^{E}(HOMO-2)*
η_{23}	0.11	1.00		
S_{21}^{N}(LUMO+1)*	0.06	0.17	1.00	
S_{28}^{E}(HOMO-2)*	0.06	0.15	0.02	1.00
ω_{22}	0.05	0.25	0.26	0.08

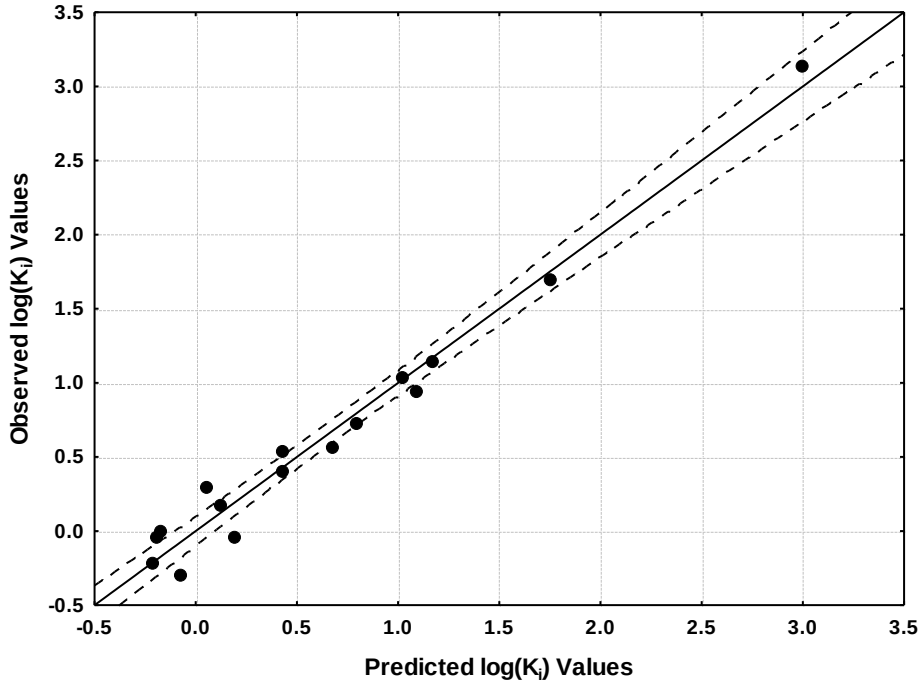

Figure 3: Plot of predicted vs. observed log(K_i) values (Eq. 1). Dashed lines denote the 95% confidence interval

The associated statistical parameters of Eq. 1 indicate that this equation is statistically significant and that the variation of the numerical values of a group of five local atomic reactivity indices of atoms of the common skeleton explains about 96% of the variation of log(K_i). Figure 3, spanning about 3.2 orders of magnitude, shows that there is a good correlation of observed *versus* calculated values and that almost all points are inside the 95% confidence interval.

Results for 5-HT_{2A} receptor affinity

The best equation obtained was:

$$\log K_i = 1.70 - 27.97F_{23}(\text{LUMO})^* + 2.21F_{23}(\text{HOMO})^* - 8.20F_{25}(\text{LUMO}+2)^* - \\ -10.93F_{29}(\text{LUMO}+2)^* + 0.58S_{20}^{N}(\text{LUMO}+2)^* - 0.39S_{11}^{E}(\text{HOMO}-2)^* \quad (2)$$

with n=16, adj-R^2=0.96, F(6,9)=63.07 (p<0.000001) and SD=0.12. No outliers were detected and no residuals fall outside the ±2σ limits. Here,F_{23}(LUMO)* is the electron population of the lowest empty MO localized on atom 23, F_{23}(HOMO)* is the electron population of the highest occupied MOI localized on atom 23, F_{25}(LUMO+2)* is the electron population of the third lowest empty MO localized on atom 25, F_{29}(LUMO+2)* is the electron population if the third lowest empty MO localized on atom 29, S_{20}^{N}(LUMO+2)* is the nucleophilic superdelocalizability of the third lowest empty MO localized on atom 20 and S_{11}^{E}(HOMO-2)* is the electrophilic superdelocalizability of the third highest occupied MO localized on atom 11.Tables 5 and 5 show the beta coefficients, the results of the t-test

for significance of coefficients and the matrix of squared correlation coefficients for the variables of Eq. 2.Figure 4 displays the plot of observed *vs.* calculated log(K_i) values.

Table 4: Beta coefficients and t-test for significance of coefficients in Eq. 2

Variable	Beta	t(9)	p-level
F_{23}(LUMO)*	-1.01	-15.57	0.000000
F_{23}(HOMO)*	0.58	8.57	0.00001
F_{25}(LUMO+2)*	-0.31	-5.69	0.0003
F_{29}(LUMO+2)*	-0.27	-4.79	0.001
S_{20}^{N}(LUMO+2)*	0.18	3.42	0.008
S_{11}^{E}(HOMO-2)*	-0.14	-2.47	0.04

Table 5: Matrix of squared correlation coefficients for the variables in Eq. 2

	F_{23}(LUMO)*	F_{23}(HOMO)*	F_{25}(LUMO+2)*	F_{29}(LUMO+2)*	S_{20}^{N}(LUMO+2)*
F_{23}(HOMO)*	0.36	1.00			
F_{25}(LUMO+2)*	0.07	0.03	1.00		
F_{29}(LUMO+2)*	0.00	0.00	0.01		
S_{20}^{N}(LUMO+2)*	0.03	0.12	0.00	0.01	1.00
S_{11}^{E}(HOMO-2)*	0.01	0.04	0.02	0.14	0.00

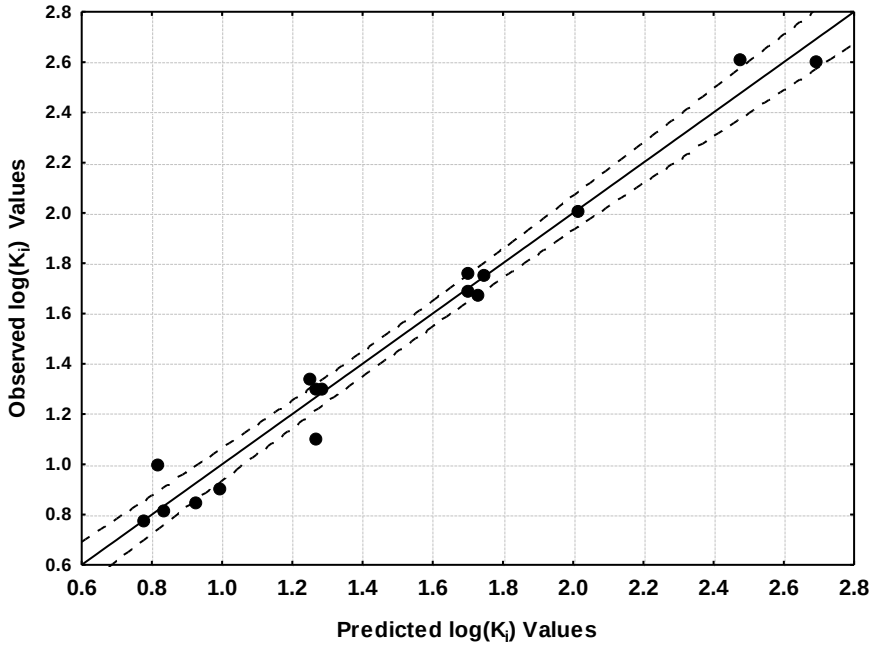

Figure 4: Plot of predicted vs. observed log(K_i) values (Eq. 2). Dashed lines denote the 95% confidence interval

The associated statistical parameters of Eq. 2 indicate that this equation is statistically significant and that the variation of the numerical values of a group of six local atomic reactivity indices of atoms of the common skeleton explains about 96% of the variation of log(K_i). Figure 4, spanning about 2 orders of magnitude, shows that there is a good correlation of observed *versus* calculated values and that almost all points are inside the 95% confidence interval.

Note that when a local atomic reactivity index of an inner occupied MO (i.e., HOMO-1 and/or HOMO-2) or of a higher vacant MO (LUMO+1 and/or LUMO+2) appears in any equation, this means that the remaining of the upper occupied MOs (for example, if HOMO-2 appears, upper means HOMO-1 and HOMO) or the remaining of the empty MOs (for example, if LUMO+1 appears, lower means the LUMO) contribute to the interaction. Their absence

in the equation only means that the variation of their numerical values does not account for the variation of the numerical value of the biological property.

Table 6: Local molecular orbitals of atoms 11, 20, 21 and 22

Mol.	Atom 11 (C)	Atom 20 (N)	Atom 21 (C)	Atom 22 (C)
1 (120)	115π116π118π-	117lp119σ120σ-	114σ119σ120σ-	114σ119σ120σ-
	121π122π123π	132σ133σ135σ	125σ133σ137σ	132σ133σ134σ
2 (120)	115π116π117π-	111σ114lp119σ-	114σ119σ120σ-	111σ114σ119σ-
	121π122π123π	135lp140lp141σ	131σ133σ137σ	131σ133σ136σ
3 (120)	114π116π117π-	110σ111σ119σ-	111σ119σ120σ-	111σ115σ119σ-
	121π122π123π	140lp142σ144σ	132σ138σ139σ	131σ132σ133σ
4 (129)	124π125π127π-	126lp128σ129σ-	123σ128σ129σ-	123σ128σ129σ-
	130π131π132π	141σ142σ144lp	134σ142σ146σ	141σ142σ143σ
5 (129)	124π125π127π-	117σ118σ128σ-	123σ128σ129σ-	119σ123σ128σ-
	130π131π132π	141σ149lp150σ	141σ142σ146σ	141σ143σ146σ
6 (116)	111π112π114π-	107σ110σ115σ-	110σ115σ116σ-	107σ110σ115σ-
	117π118π119π	130lp131lp137lp	128σ129σ132σ	126σ128σ129σ
7 (128)	124π125π126π-	119σ127σ128σ-	119σ127σ128σ-	123σ127σ128σ-
	129π130π132π	143lp148lp151lp	138σ140σ144σ	136σ138σ140σ
8 (120)	115π116π117π-	114lp118lp119σ-	114σ119σ120σ-	111σ114σ119σ-
	121π122π123π	135lp136lp140lp	133σ139σ140σ	133σ134σ140σ
9 (124)	121π122π123π-	115σ117σ122σ-	122σ123σ124σ-	117σ122σ124σ-
	125π126π128π	132lp138lp139lp	134σ137σ139σ	128σ132σ137σ
10 (123)	120π122π123π-	114σ115σ123σ-	118σ122σ123σ-	118σ123σ124σ-
	125π126π127π	131σ136lp138lp	134σ137σ138σ	131σ134σ137σ
11 (124)	120π122π123π-	114σ115σ123σ-	121σ122σ123σ-	115σ123σ124σ-
	125π126π127π	131σ135lp137lp	134σ138σ144σ	131σ136σ138σ
12 (133)	130π131π132π-	122σ131σ132σ-	131σ132σ133σ-	131σ132σ133σ-
	134π135π138π	141σ147lp148σ	143σ146σ148σ	137σ141σ146σ
13 (133)	129π131π132π-	122σ131σ132σ-	122σ131σ132σ-	131σ132σ133σ-
	134π135π137π	141σ146lp147lp	145σ147σ153σ	141σ147σ149σ
14 (120)	116π118π119π-	111σ118σ119σ-	113σ118σ119σ-	118σ119σ120σ-
	121π122π123π	127σ131lp134σ	129σ133σ134σ	127σ129σ133σ
15 (132)	130π131π132-	123σ131σ132σ-	130σ131σ132σ-	127σ131σ132σ-
	133π134π137π	139σ145lp146σ	146σ153σ154σ	139σ141σ145σ
16 (124)	119π120π122π-	114σ115σ123σ-	121σ122σ123σ-	118σ123σ124σ-
	125π126π127π	131σ135lp137σ	138σ139σ144σ	131σ133σ138σ

Table 7: Local molecular orbitals of atoms 23, 25, 28 and 29

Mol.	Atom 23 (C)	Atom 25 (C)	Atom 28 (C)	Atom 29 (C)
1 (120)	114σ119σ120σ-	114σ119σ120σ-	117π119π120π-	111π114π117π-
	136σ137σ139σ	125σ135σ136σ	124π125π127σ	124π125π127σ
2 (120)	114σ119σ120σ-	114σ119σ120σ-	114σ118π120π-	114 π 118π120π-
	126σ128σ133σ	135σ137σ140σ	125π126π135π	125π126π137π
3 (120)	115σ119σ120σ-	115σ119σ120σ-	115σ118π120π-	111σ115π118π-
	126σ128σ135σ	139σ140σ141σ	124π126π131π	124π126π134σ
4 (129)	123σ128σ129σ-	123σ128σ129σ-	126π128π129π-	122σ123π126π-

	146σ148σ149σ	134σ144σ145σ	133σ134σ136π	133π134π136σ
5 (129)	123σ128σ129σ- 134σ138σ142σ	123σ128σ129σ- 143σ145σ147σ	123π126π129π- 133π134π136σ	121σ126π129π- 133π134π136π
6 (116)	110σ115σ116σ- 120σ122σ124σ	110σ115σ116σ- 131σ135σ136σ	110π113π116π- 120π122π126σ	110π113π116π- 120π122π126σ
7 (128)	123σ127σ128σ- 131σ132σ141σ	123σ127σ128σ- 143σ144σ147σ	123π127π 128π - 131π132π138σ	122π123π127π- 131π132π133π
8 (120)	114σ119σ120σ- 125σ130σ135σ	114σ119σ120σ- 130σ136σ137σ	114π118π120π- 125π126π128π	114π118π120π- 124π 125π126π
9 (124)	117σ122σ124σ- 136σ137σ138σ	122σ123σ124σ- 128σ131σ132σ	117σ120π124π- 127π128π131π	120π122π 124π- 127π128π131π
10 (124)	115σ118σ123σ- 137σ140σ142σ	115σ118σ124σ- 129σ131σ134σ	118σ121π124π- 128π129π137π	118π121π124π- 128π129π138σ
11 (124)	115σ118σ123σ- 136σ138σ144σ	118σ121σ124σ- 129σ131σ136σ	118σ121π124π- 128π129π138σ	118π121π124π- 128π129π134π
12 (133)	131σ132σ133σ- 145σ146σ147σ	131σ132σ133σ- 137σ139σ141σ	126σ129π133π- 136π 137π139π	131π 132π 133π- 136π137π139σ
13 (133)	126σ131σ132σ- 145σ147σ148σ	126σ130σ133σ- 138σ141σ145σ	126π130π133π- 136π138π148σ	126σ130π133π- 136π138π139 π
14 (120)	113σ118σ119σ- 129σ133σ135σ	113σ117σ120σ- 124σ125σ127σ	113π117π120π- 124π125π129σ	113π117π120π- 124π125π129σ
15 (132)	123σ131σ132σ- 141σ144σ145σ	130σ131σ132σ- 136σ139σ141σ	127π131σ132σ- 135π136π141σ	127π131π132π- 135π136π141σ
16 (124)	115σ118σ123σ- 138σ142σ144σ	118σ121σ124σ- 128σ131σ133σ	118π121π124π- 128π129π133σ	118π121π124π- 128π129π133σ

Discussion

Molecular electrostatic potential (MEP)

Figure 5 shows the MEP map of molecules 1 and 9 calculated at 4.5 Å from the nuclei. Figure 6 shows the MEP map of molecules 5 and 13 calculated at 4.5 Å from the nuclei.

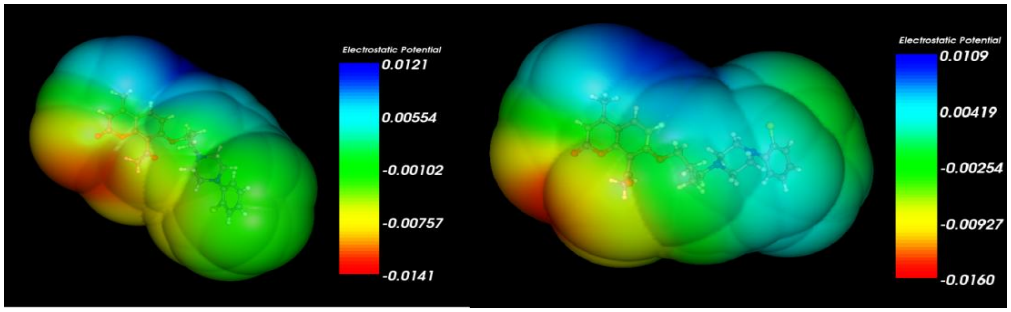

Figure 5: Molecular electrostatic potential map of molecules 1 (left) and 9 (right) at 4.5 Å of the nuclei

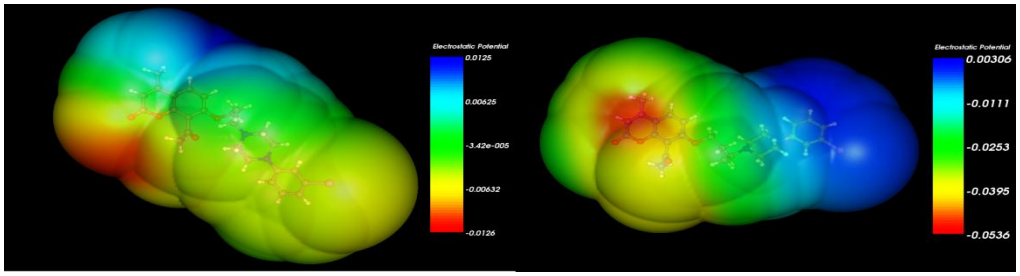

Figure 6: Molecular electrostatic potential map of molecules 5 (left) and 13 (right) at 4.5 Å of the nuclei

We can see that the oxygen atoms of rings A and B produce the stronger negative MEP volume. 4.5 Å is the zone of weak/medium drug-receptor interactions[26]. Here, the orientation and guiding processes begins. There are slight variations in the value of the MEP in the vicinity of rings C and D. For this reason, we tentatively suggest that these molecules approach their receptors with the negative MEP area of the oxygen atoms pointing toward them. Figure 7 shows the MEP map of molecules 1 and 9 (yellow isosurface = +0.0004, orange isosurface = -0.0004)[67]. Figure 8 shows the MEP map of molecules 5 and 13 (yellow isosurface = +0.0004, orange isosurface = -0.0004).

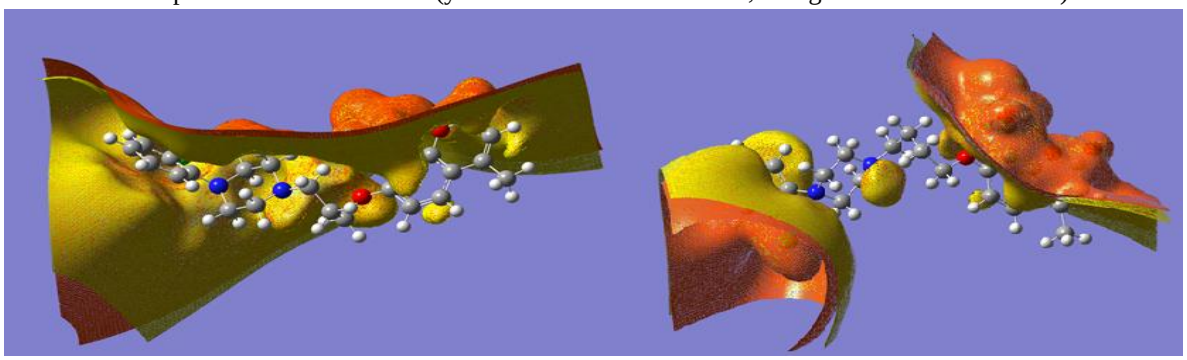

Figure 7: MEP map of molecules 1 (left) and 9 (right)

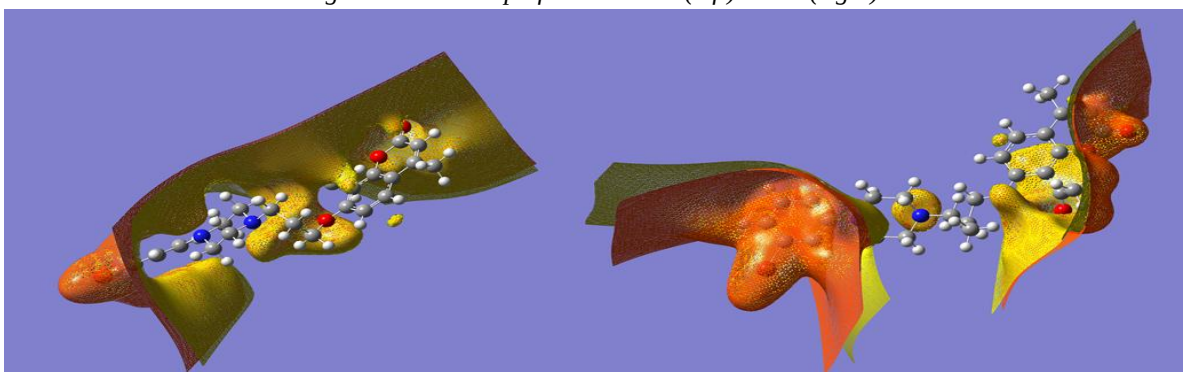

Figure 8: MEP map of molecules 5 (left) and 13 (right)

First of all, we must keep in mind that the MEP is calculated for the *in vacuo* optimized geometry. Figures 7 (left) and 8 (left) show that a continuous surface of negative MEP (orange color) exists in all the upper part of these molecules. The continuity is due to the particular conformation of the chain joining rings A-B with rings C-D (Fig. 2). This continuity is broken in the case of molecules 9 (Fig. 7, right) and 13 (Fig. 8, right) only because of the different conformation of the linker. Figure 9 shows molecules 1 and 9 with the A-B rings superimposed.

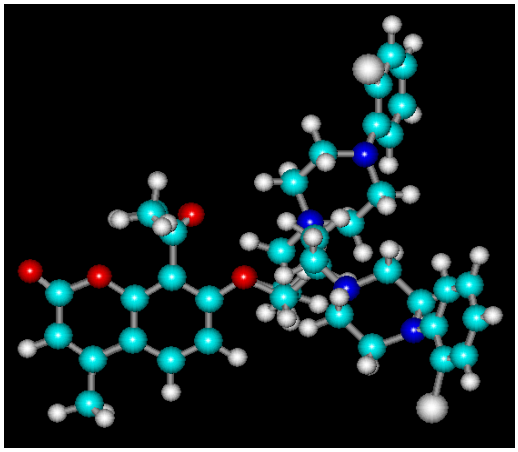

Figure 9: Molecules 1 and 9 in their lowest energy conformation with their A-B rings superimposed

Considering that the insertion of substituents was in ring D, the MEP map around rings A-B remained more or less similar in all molecules. This, again, can be taken as additional support for the suggestion that these molecules could approach their receptor with the rings A-B pointing toward them. Figures 10 and 11 show, respectively, the superimposition of the ten lowest energy conformers of molecules 1 and 9 (with MarvinView and Dreiding force field [69]).

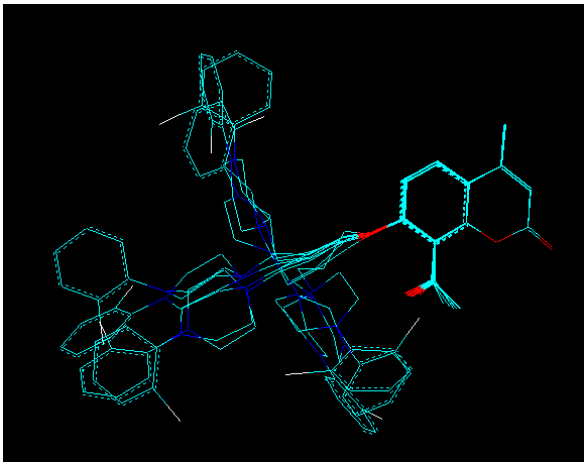

Figure 10: Superimposition of the lowest energy conformers of molecule 1. Rings A-B are at the right side

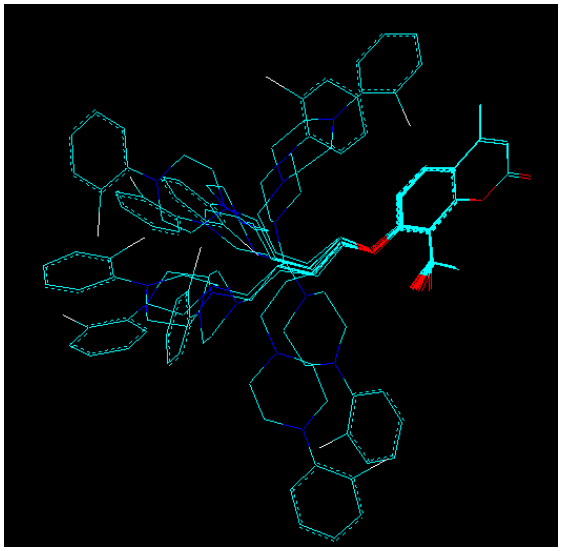

Figure 11: Superimposition of the lowest energy conformers of molecule 9. Rings A-B are at the right side

We can see that in molecule 1 there are three kinds of conformers: a group of extended conformers and two groups of conformers in which the linking chain and rings C-D are folded in opposite directions. In the case of molecule 9, given the longer length of the linker, we can distinguish the same three groups but also one conformer with the ring D facing rings A-B and other conformer that has rings C-D folded with ring D approaching rings A-B. These differences suggest that the experimentalist should select the molecules with n=3 to substitute them in rings A-B and also introduce methyl groups in ring C.

Discussion of 5-HT$_{1A}$ receptor affinity results

Table 2 shows that the importance of variables in Eq. 1 is F_{23}(LUMO+1)*>> S_{21}^{N}(LUMO+1)*> η_{23}> ω_{22}= S_{28}^{E}(HOMO-2)*.The analysis of Eq. 1 indicates that a high receptor affinity activity is associated with small (positive) values for F_{23}(LUMO+1)* and η_{23}, high (positive) values for S_{21}^{N}(LUMO+1)*, high (negative) values for

S_{28}^{E}(HOMO-2)* and high (positive) values for ω_{22}[26].Atom 23 is a carbon in ring C (Fig. 2). Table 7 shows that all local MOs have σ nature, that $HOMO_{23}^{*}$ coincides with the molecular HOMO or (HOMO-1), and that $LUMO_{23}^{*}$ corresponds to a molecular orbital energetically far from the molecular LUMO. This indicates that this atom is not prone to interact with electrons donors. Now, considering that a high receptor affinity activity is associated with small positive values for F_{23}(LUMO+1)*, then we can increase the receptor affinity by making F_{23}(LUMO+1)*=0, i.e., by changing the actual $(LUMO+)_{23}^{*}$ by a higher empty molecular MO. This provokes also a decrease of the electron-accepting capacity of this atom. This suggests that atom 23 is interacting with an electron-deficient center. The requirement of small values for η_{23} is contradictory with the just mentioned requirements. As Table 2 shows, the statistical significance of η_{23} is considerably lesser than the statistical significance of F_{23}(LUMO+1)*. Therefore, we may discard η_{23} for the discussion. Atom 21 is a carbon in ring C (Fig. 2). Table 6 shows that all local MOs have σ nature, that $HOMO_{21}^{*}$ coincides with the molecular HOMO or (HOMO-1), and that $LUMO_{21}^{*}$ corresponds to a molecular orbital energetically far from the molecular LUMO. In this case, high (positive) values for S_{21}^{N}(LUMO+1)* are associated with high affinity. This means that this atom is not prone to interact with electrons. Therefore we suggest that atom 21 is interacting with an electron deficient center. Atom 28 is a carbon in ring D (Fig. 2). Table 7 shows that all local frontier MOs have a π nature. Table 7 also shows that the local HOMO* coincides with the molecular HOMO and that the local LUMO* does not. This means that atom 28 is not a good electron acceptor. High (negative) values for S_{28}^{E}(HOMO-2)* are associated with great affinity. To get these values we must move upwards the $(HOMO-2)_{22}^{*}$ energy, making this atom more prone to share its electrons. Therefore we suggest that this atom is interacting with an electron-deficient center. Atom 22 is a carbon in ring C (Fig. 2). Table 6 shows that all MOs have a σ nature, that the local $HOMO_{22}^{*}$ coincides with the molecular HOMO or (HOMO-1) and that the local $LUMO_{22}^{*}$ coincides with molecular MOs that are energetically very far from the molecular LUMO. High (positive) values for the local atomic electrophilicity of atom 22, ω_{22}, are associated with high affinity. ω_{22} is defined as:

$$\omega_{22} = \frac{\mu_{22}^{2}}{2\eta_{22}} \qquad (3)$$

where μ_{22} is the local atomic electronic chemical potential of atom 22 and η_{22} its local atomic hardness. Higher values can be obtained faster if we force (by substitutions) the $LUMO_{22}^{*}$ to coincide with the molecular LUMO. This is so because the local atomic hardness will diminish and the local atomic electronic chemical potential will become more negative. Therefore this atom will become more prone to accept electrons suggesting that this atom is interacting with an electron-rich site.All these suggestions are displayed in the partial 2D pharmacophore of Fig. 12.

Figure 12: Partial 2D pharmacophore for 5-HT_{1A} receptor affinity

Discussion of 5-HT_{2A} receptor affinity results

Table 4 shows that the importance of variables in Eq. 2 is F_{23}(LUMO)*>> F_{23}(HOMO)*> F_{25}(LUMO+2)*> F_{29}(LUMO+2)*> S_{20}^{N}(LUMO+2)*> S_{11}^{E}(HOMO-2)*.The analysis of Eq. 2 indicates that a high receptor affinity

activity is associated with high (positive) values for F_{23}(LUMO)*, F_{25}(LUMO+2)* and F_{29}(LUMO+2)*, with small (positive) values for F_{23}(HOMO)* and S_{20}^{N}(LUMO+2)* and with small (negative) values for S_{11}^{E}(HOMO-2)*.Atom 23 is a carbon in ring C (Fig. 2). Table 7 shows that all local MOs have σ nature, that $HOMO_{23}^{*}$ coincides with the molecular HOMO or (HOMO-1), and that $LUMO_{23}^{*}$ corresponds to a molecular orbital energetically far from the molecular LUMO. A high affinity is associated with high (positive) values for F_{23}(LUMO)* and small (positive) values for F_{23}(HOMO)*. High positive values for F_{23}(LUMO)* indicate that this atom should behave as a good electron acceptor or be able to interact with electron-deficient centers. In the case of $HOMO_{23}^{*}$ the limit case to diminish the value of F_{23}(HOMO)* is simply by suppressing the localization of this MO on atom 23, replacing it by an inner occupied molecular MO (i.e., a new $HOMO_{23}^{*}$). Therefore, we suggest that atom 23 is interacting with an electron-rich center. Atom 25 is a carbon in ring C (Fig. 2). Table 7 shows that all local MOs have σ nature, that $HOMO_{25}^{*}$ coincides with the molecular HOMO and that $LUMO_{25}^{*}$ corresponds to a molecular orbital energetically far from the molecular LUMO. A high affinity is associated with high (positive) values for F_{25}(LUMO+2)*.As the presence of $(LUMO+2)_{25}^{*}$ indicates that $(LUMO+1)_{25}^{*}$ and $LUMO_{25}^{*}$ also participate in the interaction, we suggest that this atom is facing and interacting with an electron-donor site with a relatively large electron population. Atom 29 is a carbon in ring D (Fig. 2). Table 7 shows that all local frontier MOs have a π nature. In most molecules, $HOMO_{29}^{*}$ coincides with the molecular HOMO but in other cases with inner occupied molecular MOs. $LUMO_{29}^{*}$ corresponds to a molecular orbital energetically far from the molecular LUMO. A high affinity is associated with high (positive) values for F_{29}(LUMO+2)*. As in the case of atom 25, we suggest that atom 29 is also interacting with an electron-donor site. Atom 20 is one of the nitrogen atoms in ring C (Fig. 2). Table6 shows that the local HOMO, $HOMO_{20}^{*}$, coincides with one of the three highest occupied MOs of the molecules and that it has a σ nature. $LUMO_{20}^{*}$ has a σ or lone pair (lp) nature and it corresponds to a molecular orbital energetically far from the molecular LUMO in all cases. Small (positive) values for S_{20}^{N}(LUMO+2)* are associated with high affinity. These values are obtained by shifting upwards the MO energy, making this atom less prone to receive electrons. Therefore, it is suggested that this atom is interacting with an electron-deficient center. Atom 11 is a carbon in ring B (Fig. 2). Table 6 shows that all local frontier MOs have a π nature. A high affinity is associated with small (negative) values for S_{11}^{E}(HOMO-2)*, values that are obtained by shifting downwards the MO energy. This suggests that this atom should behave as a bad electron donor. Considering that $HOMO_{11}^{*}$ corresponds to one of the three highest occupied molecular MOs and that $LUMO_{11}^{*}$ coincides with the molecular LUMO in all but one case, we suggest that this 11 is interacting with an electron-rich center.All the suggestions are displayed in the partial 2D pharmacophore of Fig. 13.

Figure 13: Partial 2D pharmacophore for 5-HT_{2A} receptor affinity

It is interesting to note that in the case of the 5-HT_{1A} receptor, there are at least three carbon atoms of ring C that seem to interact with a site in the receptor. These interactions can be weak π-σ interactions between a C-H group and

a π ring system or weak interactions between occupied and empty sigma MOs. In the case of the 5-HT_{2A} receptor the situation is analogous: there are at least three atoms of ring C interacting with a site of this receptor, and the possible interactions are analogous to the 5-HT_{1A} case. This suggests the possible existence of a hydrophobic pocket in both receptors.

What is particularly important here is that ring C is the perfect target to try substitutions because the electronic effects cannot propagate through this saturated ring. Therefore, substituents like methyl, ethyl or similar ones (with only σ electrons) are suited for this work. Even substituents such as chlorine or bromine can provide very useful information about the kind of interactions of ring C with the putative site.

References

[1]. Ohno, Y. Chapter 18 - Serotonin Receptors as the Therapeutic Target for Central Nervous System Disorders. In *Serotonin*, Pilowsky, P. M., Ed. Academic Press: Boston, 2019; pp 369-390.

[2]. Żmudzka, E.; Sałaciak, K.; Sapa, J.; Pytka, K. Serotonin receptors in depression and anxiety: Insights from animal studies. *Life Sciences* 2018, 210, 106-124.

[3]. Sahu, A.; Gopalakrishnan, L.; Gaur, N.; Chatterjee, O.; Mol, P.; Modi, P. K.; Dagamajalu, S.; Advani, J.; Jain, S.; Keshava Prasad, T. S. The 5-Hydroxytryptamine signaling map: an overview of serotonin-serotonin receptor mediated signaling network. *Journal of Cell Communication and Signaling* 2018, 12, 731-735.

[4]. Blenau, W.; Baumann, A. *Serotonin receptor technologies*. Springer: 2015.

[5]. Gómez-Jeria, J. S.; Moreno-Rojas, C.; Castro-Latorre, P. A note on the binding of N-2-methoxybenzyl-phenethylamines (NBOMe drugs) to the 5-HT_{2C} receptors. *Chemistry Research Journal* 2018, 3, 169-175.

[6]. Gómez-Jeria, J. S.; Castro-Latorre, P.; Moreno-Rojas, C. Dissecting the drug-receptor interaction with the Klopman-Peradejordi-Gómez (KPG) method. II. The interaction of 2,5-dimethoxyphenethylamines and their N-2-methoxybenzyl-substituted analogs with 5-HT_{2A} serotonine receptors. *Chemistry Research Journal* 2018, 4, 45-62.

[7]. Gómez-Jeria, J. S.; Moreno-Rojas, C. Dissecting the drug-receptor interaction with the Klopman-Peradejordi-Gómez (KPG) method. I. The interaction of 2,5-dimethoxyphenethylamines and their N-2-methoxybenzyl-substituted analogs with 5-HT1A serotonine receptors. *Chemistry Research Journal* 2017, 2, 27-41.

[8]. Gómez-Jeria, J. S.; Becerra-Ruiz, M. B. Electronic structure and rat fundus serotonin receptor binding affinity of phenetylamines and indolealkylamines. *International Journal of Advances in Pharmacy, Biology and Chemistry* 2017, 6, 72-86.

[9]. Gómez-Jeria, J. S.; Abuter-Márquez, J. A Theoretical Study of the Relationships between Electronic Structure and 5-HT_{1A} and 5- HT_{2A} Receptor Binding Affinity of a group of ligands containing an isonicotinic nucleus. *Chemistry Research Journal* 2017, 2, 198-213.

[10]. Gómez-Jeria, J. S.; Robles-Navarro, A. A Quantum Chemical Study of the Relationships between Electronic Structure and cloned rat 5-HT_{2C} Receptor Binding Affinity in N-Benzylphenethylamines. *Research Journal of Pharmaceutical, Biological and Chemical Sciences* 2015, 6, 1358-1373.

[11]. Gómez-Jeria, J. S.; Robles-Navarro, A. DFT and Docking Studies of the Relationships between Electronic Structure and 5-HT_{2A} Receptor Binding Affinity in N-Benzylphenethylamines. *Research Journal of Pharmaceutical, Biological and Chemical Sciences* 2015, 6, 1811-1841.

[12]. Gómez-Jeria, J. S.; Robles-Navarro, A. A Note on the Docking of some Hallucinogens to the 5-HT_{2A} Receptor. *Journal of Computational Methods in Molecular Design* 2015, 5, 45-57.

[13]. Gómez-Jeria, J. S.; Robles-Navarro, A. A Density Functional Theory and Docking study of the Relationships between Electronic Structure and 5-HT_{2B} Receptor Binding Affinity in N-Benzyl Phenethylamines. *Der Pharma Chemica* 2015, 7, 243-269.

[14]. Gómez-Jeria, J. S.; Cassels, B. K.; Saavedra-Aguilar, J. C. A quantum-chemical and experimental study of the hallucinogen (±)-1-(2,5-dimethoxy-4-nitrophenyl)-2-aminopropane (DON). *European Journal of Medicinal Chemistry* 1987, 22, 433-437.

[15]. Gómez-Jeria, J. S.; Morales-Lagos, D.; Cassels, B. K.; Saavedra-Aguilar, J. C. Electronic structure and serotonin receptor binding affinity of 7-substituted tryptamines. *Quantitative Structure-Activity Relationships* 1986, 5, 153-157.

[16]. Gómez-Jeria, J. S.; Cassels, B. K.; Clavijo, R. E.; Vargas, V.; Quintana, R.; Saavedra-Aguilar, J. C. Spectroscopic characterization of a new hallucinogen: 1-(2,5-dimethoxy-4-nitrophenyl)-2-aminipropane (DON). *Microgram (DEA)* 1986, 19, 153-162.

[17]. Gómez-Jeria, J. S.; Morales-Lagos, D.; Rodriguez-Gatica, J. I.; Saavedra-Aguilar, J. C. Quantum-chemical study of the relation between electronic structure and pA2 in a series of 5-substituted tryptamines. *International Journal of Quantum Chemistry* 1985, 28, 421-428.

[18]. Gómez-Jeria, J. S.; Morales-Lagos, D. R. Quantum chemical approach to the relationship between molecular structure and serotonin receptor binding affinity. *Journal of Pharmaceutical Sciences* 1984, 73, 1725-1728.

[19]. Gómez-Jeria, J. S.; Morales-Lagos, D. The mode of binding of phenylalkylamines to the Serotonergic Receptor. In *QSAR in design of Bioactive Drugs*, Kuchar, M., Ed. Prous, J.R.: Barcelona, Spain, 1984; pp 145-173.

[20]. Gómez-Jeria, J. S. Approximate Molecular Electrostatric Potentials of Protonated Mescaline Analogues. *Acta sud Americana de Química* 1984, 4, 1-9.

[21]. Ostrowska, K.; Grzeszczuk, D.; Głuch-Lutwin, M.; Gryboś, A.; Siwek, A.; Leśniak, A.; Sacharczuk, M.; Trzaskowski, B. 5-HT1A and 5-HT2A receptors affinity, docking studies and pharmacological evaluation of a series of 8-acetyl-7-hydroxy-4-methylcoumarin derivatives. *Bioorganic & Medicinal Chemistry* 2018, 26, 527-535.

[22]. Gómez-Jeria, J. S. 45 Years of the KPG Method: A Tribute to Federico Peradejordi. *Journal of Computational Methods in Molecular Design* 2017, 7, 17-37.

[23]. Gómez-Jeria, J. S. Modeling the Drug-Receptor Interaction in Quantum Pharmacology. In *Molecules in Physics, Chemistry, and Biology*, Maruani, J., Ed. Springer Netherlands: 1989; Vol. 4, pp 215-231.

[24]. Gómez-Jeria, J. S.; Ojeda-Vergara, M. Parametrization of the orientational effects in the drug-receptor interaction. *Journal of the Chilean Chemical Society* 2003, 48, 119-124.

[25]. Gómez-Jeria, J. S. A New Set of Local Reactivity Indices within the Hartree-Fock-Roothaan and Density Functional Theory Frameworks. *Canadian Chemical Transactions* 2013, 1, 25-55.

[26]. Gómez-Jeria, J. S.; Kpotin, G. Some Remarks on The Interpretation of The Local Atomic Reactivity Indices Within the Klopman-Peradejordi-Gómez (KPG) Method. I. Theoretical Analysis. *Research Journal of Pharmaceutical, Biological and Chemical Sciences* 2018, 9, 550-561.

[27]. Gómez-Jeria, J. S.; Espinoza, L. Quantum-chemical studies on acetylcholinesterasa inhibition. I. Carbamates. *Journal of the Chilean Chemical Society* 1982, 27, 142-144.

[28]. Gómez-Jeria, J. S.; Sotomayor, P. Quantum chemical study of electronic structure and receptor binding in opiates. *Journal of Molecular Structure: THEOCHEM* 1988, 166, 493-498.

[29]. Gómez-Jeria, J. S.; Ojeda-Vergara, M.; Donoso-Espinoza, C. Quantum-chemical Structure-Activity Relationships in carbamate insecticides. *Molecular Engineering* 1995, 5, 391-401.

[30]. Gómez-Jeria, J. S.; Ojeda-Vergara, M. Electrostatic medium effects and formal quantum structure-activity relationships in apomorphines interacting with D1 and D2 dopamine receptors. *International Journal of Quantum Chemistry* 1997, 61, 997-1002.

[31]. Gómez-Jeria, J. S.; Lagos-Arancibia, L. Quantum-chemical structure-affinity studies on kynurenic acid derivatives as Gly/NMDA receptor ligands. *International Journal of Quantum Chemistry* 1999, 71, 505-511.

[32]. Gómez-Jeria, J. S.; Lagos-Arancibia, L.; Sobarzo-Sánchez, E. Theoretical study of the opioid receptor selectivity of some 7-arylidenenaltrexones. *Boletin de la Sociedad Chilena de Quimica* 2003, 48, 61-66.

[33]. Gómez-Jeria, J. S.; Soto-Morales, F.; Larenas-Gutierrez, G. A Zindo/1 Study of the Cannabinoid-Mediated Inhibition of Adenylyl Cyclase. *Iranian International Journal of Science* 2003, 4, 151-164.

[34]. Gómez-Jeria, J. S.; Gerli-Candia, L. A.; Hurtado, S. M. A structure-affinity study of the opioid binding of some 3-substituted morphinans. *Journal of the Chilean Chemical Society* 2004, 49, 307-312.

[35]. Gómez-Jeria, J. S.; Soto-Morales, F.; Rivas, J.; Sotomayor, A. A theoretical structure-affinity relationship study of some cannabinoid derivatives. *Journal of the Chilean Chemical Society* 2008, 53, 1393-1399.

[36]. Gómez-Jeria, J. S. A DFT study of the relationships between electronic structure and peripheral benzodiazepine receptor affinity in a group of N,N-dialkyl-2- phenylindol-3-ylglyoxylamides (Erratum in: J. Chil. Chem. Soc., 55, 4, IX, 2010). *Journal of the Chilean Chemical Society* 2010, 55, 381-384.

[37]. Bruna-Larenas, T.; Gómez-Jeria, J. S. A DFT and Semiempirical Model-Based Study of Opioid Receptor Affinity and Selectivity in a Group of Molecules with a Morphine Structural Core. *International Journal of Medicinal Chemistry* 2012, 2012 Article ID 682495, 1-16.

[38]. Gómez-Jeria, J. S. A quantum-chemical analysis of the relationships between hCB2 cannabinoid receptor binding affinity and electronic structure in a family of 4-oxo-1,4-dihydroquinoline-3-carboxamide derivatives. *Der Pharmacia Lettre* 2014, 6., 95-104.

[39]. Gómez-Jeria, J. S. A quantum chemical analysis of the relationships between electronic structure, PAK1 inhibition and MEK phosphorylation in a series of 2-arylamino-4-aryl-pyrimidines. *SOP Transactions on Physical Chemistry* 2014, 1, 10-28.

[40]. Gómez-Jeria, J. S.; Valdebenito-Gamboa, J. A DFT Study of the Relationships between the Electronic Structures of a series of 2,4,5- Trisubstituted Pyrimidines and their Inhibition of four Cyclin-dependent Kinases and their Anti-Proliferative Action against HCT-116 and MCF-7 Cell Lines. *Der Pharma Chemica* 2014, 6, 383-406.

[41]. Salgado-Valdés, F.; Gómez-Jeria, J. S. A Theoretical Study of the Relationships between Electronic Structure and CB1 and CB2 Cannabinoid Receptor Binding Affinity in a Group of 1-Aryl-5-(1-H-pyrrol-1-yl)-1-H-pyrazole-3-carboxamides. *Journal of Quantum Chemistry* 2014, 2014 Article ID 431432, 1-15.

[42]. Leal, M. S.; Robles-Navarro, A.; Gómez-Jeria, J. S. A Density Functional Study of the Inhibition of Microsomal Prostaglandin E2 Synthase-1 by 2-aryl substituted quinazolin-4(3*H*)-one, pyrido[4,3-*d*]pyrimidin-4(3*H*)-one and pyrido[2,3-*d*]pyrimidin-4(3*H*)-one derivatives. *Der Pharmacia Lettre* 2015, 7, 54-66.

[43]. Barahona-Urbina, C.; Nuñez-Gonzalez, S.; Gómez-Jeria, J. S. Model-based quantum-chemical study of the uptake of some polychlorinated pollutant compounds by Zucchini subspecies. *Journal of the Chilean Chemical Society* 2012, 57, 1497-1503.

[44]. Alarcón, D. A.; Gatica-Díaz, F.; Gómez-Jeria, J. S. Modeling the relationships between molecular structure and inhibition of virus-induced cytopathic efects. Anti-HIV and anti-H1N1 (Influenza) activities as examples. *Journal of the Chilean Chemical Society* 2013, 58, 1651-1659.

[45]. Gómez-Jeria, J. S.; Flores-Catalán, M. Quantum-chemical modeling of the relationships between molecular structure and in vitro multi-step, multimechanistic drug effects. HIV-1 replication inhibition and inhibition of cell proliferation as examples. *Canadian Chemical Transactions* 2013, 1, 215-237.

[46]. Paz de la Vega, A.; Alarcón, D. A.; Gómez-Jeria, J. S. Quantum Chemical Study of the Relationships between Electronic Structure and Pharmacokinetic Profile, Inhibitory Strength toward Hepatitis C virus NS5B Polymerase and HCV replicons of indole-based compounds. *Journal of the Chilean Chemical Society* 2013, 58, 1842-1851.

[47]. Gómez-Jeria, J. S. A Note on the Relationships between Electronic Structure and Inhibition of Chikungunya Virus Replication by a group of [1,2,3]Triazolo[4,5-d]pyrimidin-7(6H)-ones Derivatives. *Journal of Computational Methods in Molecular Design* 2014, 4, 38-47.

[48]. Muñoz-Gacitúa, D.; Gómez-Jeria, J. S. Quantum-chemical study of the relationships between electronic structure and anti influenza activity. 1. The inhibition of cytophatic effects produced by the influenza A/Guangdong Luohu/219/2006 (H1N1) strain in MDCK cells by substituted bisaryl amide compounds. *Journal of Computational Methods in Molecular Design* 2014, 4, 33-47.

[49]. Muñoz-Gacitúa, D.; Gómez-Jeria, J. S. Quantum-chemical study of the relationships between electronic structure and anti influenza activity. 2. The inhibition by 1H-1,2,3-triazole-4-carboxamide derivatives of the cytopathic effects produced by the influenza A/WSN/33 (H1N1) and A/HK/8/68 (H3N2) strains in MDCK cells. *Journal of Computational Methods in Molecular Design* 2014, 4, 48-63.

[50]. Pino-Ramírez, D. I.; Gómez-Jeria, J. S. A Quantum-chemical study of the in vitro cytotoxicity of a series of (Z)-1-aryl-3-arylamino-2-propen-1-ones against human tumor DU145 and K562 cell lines. *American Chemical Science Journal* 2014, 4, 554-575.

[51]. Gómez-Jeria, J. S. A Theoretical Study of the Relationships between Electronic Structure and Antifungal Activity against *Botrytis cinerea* and *Colletotrichum lagenarium* of a Group of Carabrone Hydrazone Derivatives. *Research Journal of Pharmaceutical, Biological and Chemical Sciences* 2015, 6, 688-697.

[52]. Gómez-Jeria, J. S.; Becerra-Ruiz, M. B. A Preliminary Quantum-Chemical Study of the anti-HIV-1 III_B Activity of a series of Etravirine-VRX-480773 Hybrids. *Der Pharma Chemica* 2015, 7, 362-369.

[53]. Gómez-Jeria, J. S.; Robles-Navarro, A. A theoretical study of the relationships between electronic structure and inhibition of tumor necrosis factor by cyclopentenone oximes. *Research Journal of Pharmaceutical, Biological and Chemical Sciences* 2015, 6, 1337-1351.

[54]. Gómez-Jeria, J. S.; Robles-Navarro, A. Quantum-chemical study of the cytotoxic activity of pyrimidine–benzimidazol hybrids against MCF-7, MGC-803, EC-9706 and SMMC-7721 human cancer cell lines. *Research Journal of Pharmaceutical, Biological and Chemical Sciences* 2015, 6, 755-783.

[55]. Gómez-Jeria, J. S.; Valdebenito-Gamboa, J. A quantum-chemical analysis of the antiproliferative activity of N-3-benzimidazolephenylbisamide derivatives against MGC803, HT29, MKN45 and SW620 cancer cell lines. *Der Pharma Chemica* 2015, 7, 103-121.

[56]. Bravo, H. R.; Weiss-López, B. E.; Valdebenito-Gamboa, J.; Gómez-Jeria, J. S. A theoretical analysis of the relationship between the electronic structure of indole derivatives and their phytotoxicity against Lactuca Sativa seeds. *Research Journal of Pharmaceutical, Biological and Chemical Sciences* 2016, 7, 792-798.

[57]. Gómez-Jeria, J. S.; Abarca-Martínez, S. A theoretical analysis of the cytotoxicity of a series of β-carboline-dithiocarbamate derivatives against prostatic cancer (DU-145), breast cancer (MCF-7), human lung adenocarcinoma (A549) and cervical cancer (HeLa) cell lines. *Der Pharma Chemica* 2016, 8, 507-526.

[58]. Gómez-Jeria, J. S.; Latorre-Castro, P. On the relationship between electronic structure and carcinogenic activity in substituted Benz[a]anthracene derivatives. *Der Pharma Chemica* 2016, 8, 84-92.

[59]. Gómez-Jeria, J. S.; Castro-Latorre, P. A Density Functional Theory analysis of the relationships between the Badger index measuring carcinogenicity and the electronic structure of a series of substituted Benz[a]anthracene derivatives. *Chemistry Research Journal* 2017, 2, 112-126.

[60]. Gómez-Jeria, J. S.; Castro-Latorre, P.; Kpotin, G. Quantum Chemical Study of the Relationships between Electronic Structure and Antiviral Activities against Influenza A H1N1, Enterovirus 71 and Coxsackie B3 viruses of some Pyrazine-1,3-thiazine Hybrid Analogues. *International Journal of Research in Applied, Natural and Social Sciences* 2017, 5, 49-64.

[61]. Note. The results presented here are obtained from what is now a routinary procedure. For this reason, we built a general model for the paper's structure. This model contains *standard* phrases for the presentation of the methods, calculations and results because they do not need to be rewritten repeatedly and the number of possible variations to use is finite. In 2017.

[62]. Frisch, M. J.; Trucks, G. W.; Schlegel, H. B.; Scuseria, G. E.; Robb, M. A.; Cheeseman, J. R.; Montgomery, J., J.A.; Vreven, T.; Kudin, K. N.; Burant, J. C.; Millam, J. M.; Iyengar, S. S.; Tomasi, J.; Barone, V.; Mennucci, B.; Cossi, M.; Scalmani, G.; Rega, N. *G03 Rev. E.01*, Gaussian: Pittsburgh, PA, USA, 2007.

[63]. Gómez-Jeria, J. S. *D-Cent-QSAR: A program to generate Local Atomic Reactivity Indices from Gaussian 03 log files. v. 1.0*, v. 1.0; Santiago, Chile, 2014.
[64]. Gómez-Jeria, J. S. An empirical way to correct some drawbacks of Mulliken Population Analysis (Erratum in: J. Chil. Chem. Soc., 55, 4, IX, 2010). *Journal of the Chilean Chemical Society* 2009, 54, 482-485.
[65]. Statsoft. *Statistica v. 8.0*, 2300 East 14 th St. Tulsa, OK 74104, USA, 1984-2007.
[66]. Gómez-Jeria, J. S. *Elements of Molecular Electronic Pharmacology (in Spanish)*. 1st ed.; Ediciones Sokar: Santiago de Chile, 2013; p 104.
[67]. Dennington, R. D.; Keith, T. A.; Millam, J. M. *GaussViev 5.0.8*, GaussViev 5.0.8, 340 Quinnipiac St., Bldg. 40, Wallingford, CT 06492, USA, 2000-2008.
[68]. Varetto, U. *Molekel 5.4.0.8*, Swiss National Supercomputing Centre: Lugano, Switzerland, 2008.
[69]. Chemaxon. *MarvinView*, 6.3.1; www.chemaxon.com: USA, 2014.